Performance Analysis of Small Horizontal Axis Wind Turbine with Airfoil NACA 4412

Syam Widiyanto[1*], Sasongko Pramonohadi[2], Mohammad Kholid Ridwan[3]

[1] Student of Master System Engineering, Faculty of Engineering
[2] Department of Electrical and Informatics, Faculty of Engineering
[3] Department of Nuclear and Physics, Faculty of Engineering
Universitas Gadjah Mada, Yogyakarta, Yogyakarta 55281, Indonesia.

[*] Corresponding author:
Email: syamwidiyanto@mail.ugm.ac.id

Abstract.

The horizontal axis wind turbine (HAWT) design with low wind speed requires blade geometry selection. The analysis uses the potential flow panel method and the integral boundary layer formulation to analyze wind flow around the airfoil. The blade design with the blade element momentum (BEM) theory has an aerodynamic coefficient value along the blade. Power wind calculates to model the wind shear pressure at each blade. This research aims to determine the wind turbine rotor based on the performance, including the power coefficient, tip speed ratio, power, and rpm. The simulation uses an airfoil NACA 4412 which has optimal coefficient lift (Cl) = 1.92 at 19^0 pitch of angle, coefficient drag (Cd) = 0.0635 at 13^0 pitch angle and Cl / Cd = 155 at tilt angle = 40. Five models of 2.5 m diameter blades with different angles for each chord. The test results show that the change in the speed ratio affects the power coefficient so that the optimal power coefficient on NACA 4412 in experiment 5 is 0.56, and change in rotation per minute affects the output power so that the rotation per minute and the optimal power in experiment 4 with a value of 374 rpm and 553 W.

Keywords: HAWT, BEM, small wind turbine, coefficient power, rpm

1. INTRODUCTION

The wind is the air that moves from high pressure to an area of low pressure. Indonesia has the potential for wind speeds ranging from 2 m / s to 6 m / s, which blow for 6 hours/day. Wind speed and variations in the number of turbine blades will affect the power generated. In a case study on the coast of Banda Aceh, windmills use horizontal turbines with various blades of 5, 6, and 7 blades made of meranti. The Data has collected to measure the wind speed, the generator shaft's rotational speed, and the resulting electric current. The results showed that wind speeds below 5 m / s are ideal for using three blades and wind speeds of more than 7 m / s are better for using blades of more than 3 [1].

The horizontal axis wind turbines improved performance to operating at low wind speeds, and then aerodynamically depends on geometry [2]. They modified rotor geometry with NACA 4415 airfoil to predict power and power coefficient, using Blade Element Momentum (BEM) based on Lifting Line Theory (LLT). Power output and

coefficients power analyzed at wind speeds of 3, 4, 5, 6, and 7 m / s. The maximum predicted power output achieved at wind speeds of 7 m / s with TSR = 6. [3] and the value of TSR = 7, and the output power is 165,924 Watt. [4]. The performance of the turbine includes power, thrust with different TSR. The turbine performance obtains a maximum power coefficient (Cp) of 0.4642 at TSR = 6, and the thrust coefficient (Ct) increases over the entire TSR range, which is evaluating a value of 0.8788 at TSR 10.

The design of wind turbine blades uses blade elements and theoretical momentum. The performance of small turbine blades is based on lift coefficient and drag coefficient at a wind speed of 8.4 m / s with a low Reynolds number to face the laminar separation effect. Low Reynolds number specially designed airfoil used for small wind turbine blades [5].

II. METHODS

The Simulation CFD analysis includes a calculate aerodynamics of a NACA-4412 airfoil in a blade design consisting of a thickness of 12% and a chamber of 4%
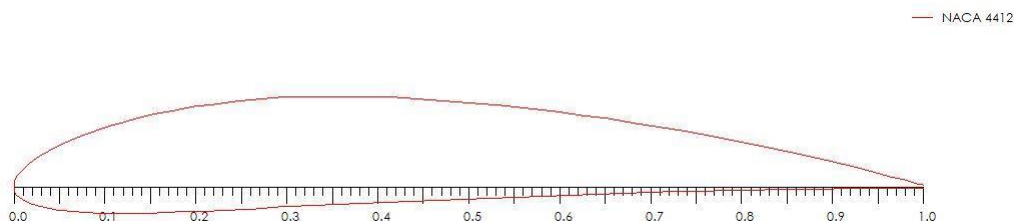

Fig 1. Cross-section of NACA-4412 airfoil

Foil Code

XFOIL combines the potential flow panel method and integral boundary layer formulation to analyze wind flow around the airfoil. XFOIL quickly predicts airfoil performance at low Reynolds number [6] and its convergence through iterations between the outer and inner flow solutions at the boundary layer's displacement thickness. Thus, the XFOIL Code calculates the condensed pressure distribution and captures the finite trailing edge and laminar bubble separation effect. XFOIL uses the eN estimate method to compute transitions. With this method, the code tracks only the most amplified frequency at a particular point in the airfoil downstream from the point of instability to obtain the noise's amplitude. The transition is assumed to be when the integrated amplitude reaches an empirically determined value. N, which is suitable for XFOIL calculations, can be calculated by equation.

$$N = -8.43 - 2.4 \ln (T_u)$$

where Tu represents the absolute turbulence intensity. In the current work, N is a default value of 9, which corresponds to the smooth wing surface in the low turbulence intensity of the freestream. [7] The turbine blade is optimized to achieve the maximum power coefficient for a given blade by k, the drag to lift coefficient, the attack angle, and the tip speed ratio. [8]. This article has used the momentum element blade theory

to find optimal values analytically. Effect of power coefficient for different angle attacks, tip speed ratio, drag coefficient ratio, and lift coefficient [9].

The blade design with the blade element momentum (BEM) theory has an aerodynamic coefficient along the blade. The turbine power has modeled the wind shear pressure at the blades. Combining the BEM theory's functions, the performance has calculated across the blade. The results showed that the wind shift had little impact on the root area's aerodynamic coefficient. [10]
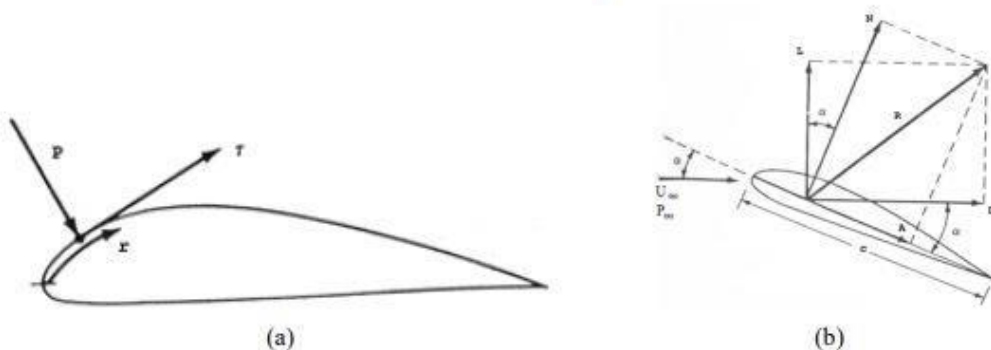
$$R_e = \frac{\rho U c}{\mu}$$

(a)   (b)

Fig 2. Schematic diagram of airfoil aerodynamics

The pressure (p) and shear force (τ) on the airfoil impact (Figure 1a) the aerodynamic force which includes normal force (N), lift (L) and drag force (D) as shown in Figure 1b. and the pressure coefficient (Cp) and the friction coefficient (Cf) has defined as:

$$C_P = \frac{P - P_\infty}{0.5 \, \rho \, U_\infty^2}$$

$$C_f = \frac{\sigma}{0.5 \, \rho \, U_\infty^2}$$

Lift force (L), drag force (D), and momentum has understood as a coefficient of lift (Cl), drag Cd), and momentum (Cm) as a function of angle of attack (α)where Cn is the typical coefficient, and Ca is the axial coefficient, then it can be obtained that the lift coefficient is:

$$C_L = \frac{F_L}{\frac{1}{2}\rho A v^2}$$

Furthermore, the drag coefficient is:

$$C_D = \frac{F_D}{\frac{1}{2}\rho A v^2}$$

Power Coefficient

A wind turbine's capacity to extract power from the wind depends on three main factors: wind speed, the wind turbine power curve, and the ability to harness energy

due to wind fluctuations. The blade has a blade element that has a degree of tilt, which will form a curve at the blade (β), then the following equation will be obtained:

$$\eta = \frac{c_l}{c_n}$$

Tip Speed Ratio

The relationship of rotation with blade radius and wind speed is an essential factor in optimizing the geometry of the horizontal axis wind turbine (HAWT); the design tip speed ratio (DTSR) [11]. It has determined as follows:

$$TSR = \frac{R\omega}{v}$$

In this test using a tip speed ratio, the rotations per minute produced by the windmill are as follows:

$$\lambda = \frac{\omega R}{v} = \frac{2\pi n R}{60\,v}$$
$$n = \frac{60\,\lambda v}{2\pi R}$$

Turbine Power

$$P_t = \frac{1}{2}\rho A v^3$$

Power coefficient

Constant wind speed produces a different power coefficient from the maximum wind speed because of the difference in tip speed ratio. Meanwhile, the rotational speed and wind speed distribution determine the range tip speed ratio. The pitch angle affects the wind turbine's aerodynamic performance with different tip speed ratios. [12]

$$Cp = \frac{T_g}{P_t}$$

Geometry horizontal axis wind turbine blade with NACA 4412

Position (m)	Chord (m)	Rotor 1 Twist	Rotor 2 Twist	Rotor 3 Twist	Rotor 4 Twist	Rotor 5 Twist
0	0,04	74,8057	72,1315	69,5043	66,9336	64,4277
0,1	0,04	56,2519	49,0989	42,96697	37,7717	33,3758
0,2	0,109091	31,2519	23,4598	17,2778	12,5581	8,88287
0,3	0,099174	21,7486	13,9977	8,61391	4,71985	1,79719
0,4	0,901578	14,7686	7,83685	3,24608	0,0186436	-2,36038
0,5	0,081962	9,72144	3,59674	0,347578	-3,07607	-5,06752
0,6	0,074578	5,96218	0,531148	-2,90342	-5,25588	-6,96273
0,7	0,067737	3,0749	-1,77642	-4,80733	-6,86996	-8,36084
0,8	0,061579	0,798422	-3,5708	-6,27754	-8,1143	-9,43357
0,9	0,055981	-1,03715	-5,00347	-7,44566	-9,09512	-10,2821
1	0,050892	-2,54573	-6,17241	-8,3954	-9,89333	-10,9698
1,1	0,046265	-39059	-7,14356	-9,18235	-10,5538	-11,5383
1,21	0,042059	-4,97119	-8,03768	-9,90536	-11,1598	-12,0587

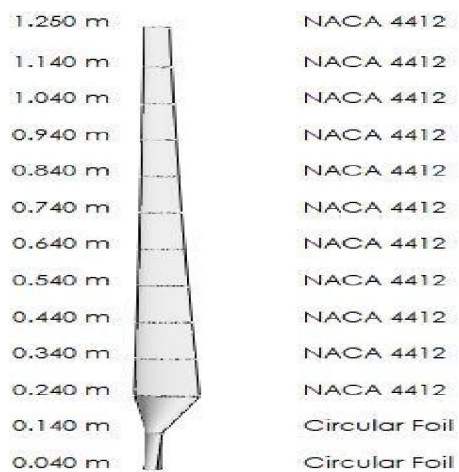**Table 1.** The geometry of wind turbine blades

Figure 3. Cross-section of the wind turbine blade

Simulation iteration

The iteration variables of the BEM method are the axial and radial induction factors as follows:

$$a = \left(\frac{4\sin^2\theta}{\sigma C_n} + 1\right)^{-1}$$

$$a' = \left(\frac{4\sin\theta\cos\theta}{\sigma C_t} - 1\right)^{-1}$$

Then the inlet flow angle θ, the tangential and normal force coefficients Ct and Cn and the rotor solidity σ, which is the part of the element blade enclosed with the blade:

$$\sigma = \frac{cB}{2\pi r}$$

Then the inlet flow angle θ, the tangential and normal force coefficients Ct and Cn and the rotor solidity σ, which is the part of the element blade enclosed with the blade:
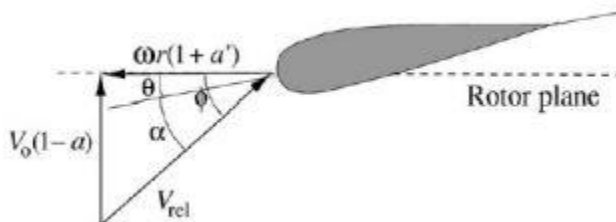

Fig. 4. Cross-section of the chord

The chord section shows the velocity in the rotor plane. If the induction factor for calculating the inlet flow angle (φ) gives the angle of attack (α), the angle between the airfoil chord line and the relative wind speed experienced with the rotating blade:

$$\alpha = \varphi - \theta$$

where $\theta = \theta_p + \beta$ is a combination of twist angle β and pitch angle θ_p. The lift and drag coefficients of the airfoil refer to the lift and drag simulation caused by the specified airfoil. The induction factor can be calculated and compared with the initial induction factor from this equation. If the max (Δa, Δa0) with the convergence criterion iterations have been calculating the next annular element.

III. RESULT AND DISCUSSION

Koefisien Lift
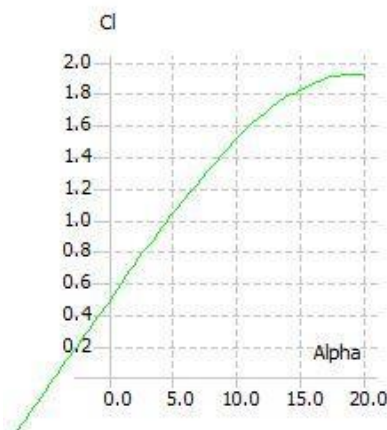
Graph.1 Lift coefficient vs. angle of attack

Lifting force simulation results at 1^0 (0.60), 2^0 (0.70), 3^0 (0.82), 4^0 (0.93), 5^0 (1.04), 6^0 (1.14), 7^0 (1.23), 8^0 (1.33), 9^0 (1.42), 10^0 (1.51), 11^0 (1.60), 12^0 (1.67), 13^0 (1.73), 14^0 (1.78), 15^0 (1.82), 16^0 (1.86), 17^0 (1.89), 18^0 (1.91), 19^0 (1.92), 20^0 (1.90). In the simulation above the highest lift at 19^0, the lift test is carried out from 1^0 to find the optimal value. The most high the value of the degree of tilt and the higher the lift.
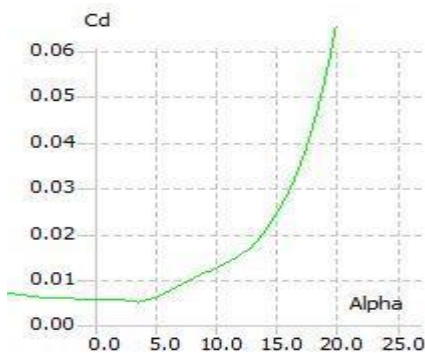

Graph 2. Coefficient of drag vs. angle of attack

Lifting force simulation results at 1^0 (0.0052), 2^0 (0.0054), 3^0 (0.0063), 4^0 (0.0074), 5^0 (0.00063), 6^0 (0.0074), 7^0 (0.0088), 8^0 (0.00102), 9^0 (0.00113), 10^0 (0.00126), 11^0 (0.0136), 12^0 (0.0155), 13^0 (0.0173), 14^0 (0, 0203), 15^0 (0.0243), 16^0 (0.0286), 17^0 (0.0348), 18^0 (0.0427), 19^0 (0.0525), 20^0 (0.0653),. In the simulation above the highest lift at 20 0, the test of lift is carried out from 10 to find the optimal value. The higher the value of the degree of tilt, the higher the lift.
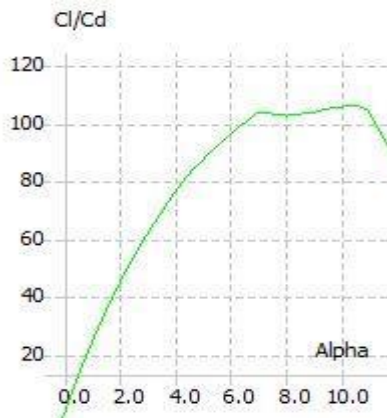
Graph 3. Cl / Cd vs. angle of attack

Graph 3. The result shows a ratio coefficient lift and drags and attack angle at 1^0 (106), 2^0 (129), 3^0(161), 4^0 (177),5^0 (170), 6^0 (154), 7^0(140), 8^0 (131), 9^0 (126), 10^0 (121),11^0 (116),12^0 (108), 13^0 (100), 14^0 (87), 15^0 (75),16^0 (64), 17^0 (54), 18^0 (44), 19^0 (36) and 20^0 (29). Cl / Cd's optimal value at an attack of 4^0, the value of lift and drag ratio is 177.

Relationship between power coefficient and tip speed ratio (TSR)
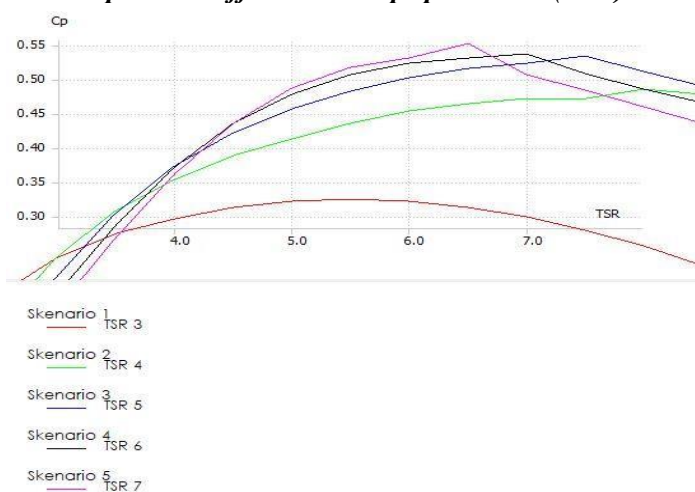
Graph 4. Power vs. TSR coefficient

Scenario 1

The table above results provides information that the higher the tip speed ratio value, the higher the power coefficient value. In this study, scenario one has detailed by producing a tip speed ratio with a power coefficient (Cp) of 0.0022, and an increase

in TSR 2 with a power coefficient (0.09), TSR 3 (0.24). TSR 4 (0.295) TSR 5 (0.32). The TSR of 6 is (0.322). TSR 7 (0.30). From TSR 8 to TSR 10, the power coefficient decreases. TSR 8 (0.26). TSR 9 (0.19). TSR 10 (0.12). At this horizontal axis wind turbine, the highest value is TSR 7 of 0.322.

Scenario 2

The test data results in scenario 2 produce data with TSR 1 to TSR 7, increasing the power coefficient. TSR affects the power coefficient. The data are as follows: TSR 1 (0.002). TSR 2 (0.007). TSR 3 (0.024). TSR 4 (0.35). TSR 5 (0.41). TSR 6 (0.45). TSR 7 (0.457). The power coefficient decreased at TSR 8 to TSR 10 (TSR 8 (0.49). TSR 9 (0.43) and TSR 10 (0.40). The highest value for TSR 7 is 0.457.

Scenario 3

The results of scenario 3 produce power coefficient data. The TSR result affects the power coefficient. Scenario 3 does by calculating TSR 1 with a power coefficient (Cp) of 0.0059, TSR 2 (0.06). TSR 3 (0.21). TSR 4, (0.37) TSR 5 (0.46). TSR 6 (0.50) and TSR 7 (0.525). At TSR 8 to TSR 10, the power coefficient decreased so that TSR 8 (0.51) and TSR 9 (0.47) TSR 10 (0.41). The highest value at the TSR 7 value is 0.525.
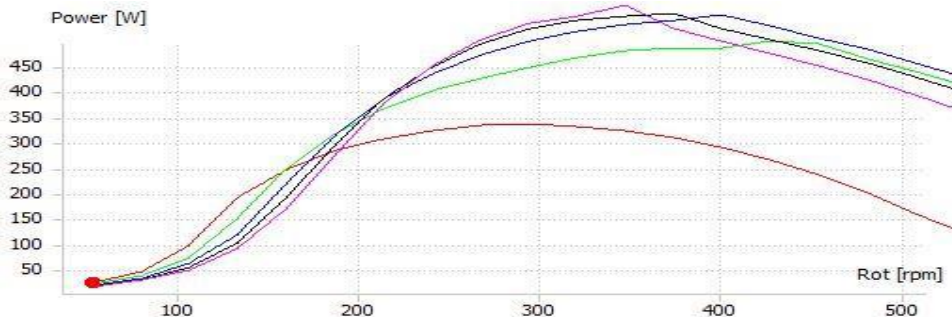
Scenario 4

Testing in scenario 4 produces data using TSR 1 to TSR 7 increases the power coefficient so that TSR 1 (0.0058), TSR 2 (0.005), TSR (0.019), TSR 4 (0.37), TSR 5 (0.48)). TSR 6 (0.52) and TSR 7 (0.53). Testing TSR 8 to TSR 10, the power coefficient has decreased. In the results of TSR (0.48), TSR 9 (0.44), TSR 10 (0.38). The highest value at the TSR 7 value is 0.53.

Scenario 5

The results of the data from scenario 5 conducted a test with the results at TSR 1 - TSR 6.5, there was an increase in the power coefficient (Cp). The following data; TSR 1 (0.0056), TSR 2 (0.004), TSR 3 (0.016), TSR 4 (0.36). TSR 5 (0.49), TSR 6 (0.53) and TSR 6.5 (0.553). Tests on TSR 7 - TSR 10, the power coefficient is getting smaller, then TSR 7 (0.50), TSR 8 (0.46), TSR 9 (0.41) and TSR 10 (0.34). The highest value in scenario 5 is a TSR value of 6.5, namely 0.553.

Power Relationship with rotations per minute (RPM)

Graph 5. Power vs. rpm

Scenario 1

TSR 1 with an RPM of 53 produces 23 W. TSR 2 with an RPM of 107 produces 97 W. TSR 3 with an RPM of 160 produces 247 W. TSR 4 with an RPM of 214 produces a power of 305 W. TSR 5 with an RPM of 267 produces 332 W. TSR 6 with an RPM of 321 produces 331 W. TSR 7 with an RPM of 374 produces 308 W. TSR 8 with an RPM of 428 produces 274 W. TSR 9 with an RPM of 481 produces 160 W. TSR 10 with an RPM of 534 producing 122 W.

Scenario 2

TSR 1 with RPM of 53 produces 20 W. TSR 2 with RPM of 107 produces 72 W. TSR 3 with RPM of 160 produces 240 W. TSR 4 with RPM of 214 produces 240 W. TSR 5 with RPM of 267 produces 426 W. TSR 6 with an RPM of 321 produces 467 W. TSR 7 with an RPM of 374 produces 485 W. TSR 8 with an RPM of 428 produces 500 W. TSR 9 with an RPM of 481 produces 464 W. TSR 10 with an RPM of 534 producing 411 W.

Scenario 3

Tests to produce a power quantity with TSR 1 - TSR 10 get an increasing power, while the power is as follows; TSR 1 with RPM 5 (18 W), TSR 2 with RPM 107 (60 W), TSR 3 with RPM 160 (220 W)), TSR 4 with RPM 214 (385 W), TSR 5 with RPM 267 produces 471 W. TSR 6 with RPM 321 (517 W). TSR 7 with RPM 374 (539 W). Testing at TSR 8 - TSR 10 experienced a decrease in power with TSR 8 RPM 428 (528 W), TSR 9 with RPM 481 (482 W). TSR 10 with RPM 534 (428 W). Optimal power occurs at TSR TSR 7 with RPM 374 (539 W).

Scenario 4

In testing, performing TSR 1 - TSR 7, the power increases. TSR with RPM 53 (17 W), TSR 2 with RPM 107 (53 W), TSR 3 with RPM 160 (193 W), TSR 4 with RPM 214 (383 W), TSR 5 with RPM 267 (492 W, TSR 6 with RPM 321 (492 W), and TSR 7 with RPM 374 (553 W). TSR 8 - TSR 10 began to decline with TSR 8 with RPM 428 (501 W). TSR 9 with RPM (456 W) and TSR 10 with RPM 534 (400 W).

Scenario 5

The data above results, the power increase from TSR 1 - TSR 7. The data obtained are as follows; TSR with RPM 53 (16 W), TSR 2 with RPM 107 (48 W). TSR 3 with RPM 160 (171 W), TSR 4 with RPM 214 (373W), TSR 5 at RPM 267 (501 W), TSR 6 with RPM 321 (548 W) and TSR 7 with RPM 374 (522 W). decreased from TSR 8-TSR10 then, TSR 8 with RPM 428 (474 W, TSR 9 with RPM 481 (423 W) and TSR 10 with RPM 534 (359 W).

IV. CONCLUSION

The coefficient lift and drag coefficient on geometry with NACA 4412 at 1^0 to 20^0 high lift and drag value. The optimal values of lift and drag are 13^0 and 20^0, respectively. Changes in the inclination angle affect the lift force and drag. The more

the value of the inclination angle, the greater the value of the tensile force (lift) and drag (drag).The ratio of lift and drag (Cl / Cd) NACA 4412 at 10 to 40 increases Cl / Cd's value and decreases so that the optimal value is determined in the Cl / Cd ratio at 40 for NACA 4412.

At tip speed ratio (TSR) 1 to TSR 7 has increased with the optimal value at TSR 7 and TSR 8 to TSR 10, there is a decrease in the power coefficient. In the windmill experiment with NACA 4412, experiment 1 with a power coefficient (0.30), experiment 2 with a power coefficient (0.46), experiment 3 with a power coefficient (0.52), experiment 4 with a power coefficient (0.53) and experiment 5 with a power coefficient (0.56). Tip speed ratio affects the change in power coefficient so that the optimal coefficient on NACA 4412 in experiment 5 is 0.56.

At tip speed ratio (TSR) 1 to TSR 7 has increased with the optimal value at TSR 7 and TSR 8 to TSR 10, there is a decrease in the power coefficient. In the windmill experiment with NACA 4412, experiment 1 with a power coefficient (0.30), experiment 2 with a power coefficient (0.46), experiment 3 with a power coefficient (0.52), experiment 4 with a power coefficient (0.53)) and experiment 5 with a power coefficient (0.56). Tip speed ratio affects the change in power coefficient so that the optimal coefficient on NACA 4412 in experiment 5 is 0.56.

REFERENCES

[1] A. Syuhada, M. I. Maulana, Syahriza, M. S. M. Sani, and R. Mamat, "The potential of wind velocity in the Banda Aceh coast to the ability to generate electrical energy by horizontal axis wind turbines," *IOP Conf. Ser. Mater. Sci. Eng.*, vol. 788, p. 012082, Jun. 2020, DOI: 10.1088/1757-899X/788/1/012082.

[2] X. Shen, H. Yang, J. Chen, X. Zhu, and Z. Du, "Aerodynamic shape optimization of non-straight small wind turbine blades," *Energy Convers. Manag.*, **vol. 119,** pp. 266–278, Jul. 2016, DOI: 10.1016/j.enconman.2016.04.008.

[3] S. Sudarsono, A. A. Susastriawan, and S. Sugianto, "Three-dimensional CFD Analysis of Performance of Small-scale Hawt based on Modified NACA-4415 Airfoil," *Int. J. Technol.*, vol. 10, no. 1, p. 212, Jan. 2019, DOI: 10.14716/ijtech.v10i1.2237.

[4] A. Sayogo and N. Caroko, "PERANCANGAN DAN PEMBUATAN KINCIR ANGIN TIPE HORIZONTAL AXIS WIND TURBINE (HAWT) UNTUK DAERAH PANTAI SELATAN JAWA," p. 8, 2016.

[5] M. R. Birajdar and S. A. Kale, "PERFORMANCE ANALYSIS OF NEW AIRFOILS AND BLADE FOR A SMALL WIND TURBINE," p. 12.

[6] S. McTavish, D. Feszty, and F. Nitzsche, "Evaluating Reynolds number effects in small-scale wind turbine experiments," *J. Wind Eng. Ind. Aerodyn.*, **vol. 120, pp. 81–90**, Sep. 2013, DOI: 10.1016/j.jweia.2013.07.006.

[7] J. Morgado, R. Vizinho, M. A. R. Silvestre, and J. C. Páscoa, "XFOIL vs. CFD performance predictions for high lift low Reynolds number airfoils," *Aerosp. Sci. Technol.*, vol. 52, pp. 207–214, May 2016, DOI: 10.1016/j.ast.2016.02.031.

[8] . R. K., "ANALYSIS AND OPTIMIZATION OF HORIZONTAL AXIS WIND TURBINE BLADE PROFILE," *Int. J. Res. Eng. Technol.*, **vol. 05,** no. 07, pp. 19–24, Jul. 2016, DOI: 10.15623/ijret.2016.0507004.

[9] B. Bavanish and K. Thyagarajan, "Optimization of power coefficient on a horizontal axis wind turbine using bem theory," *Renew. Sustain. Energy Rev.*, vol. 26, pp. 169–182, Oct. 2013, doi: 10.1016/j.rser.2013.05.009.

[10] S. Rajakumar and D. Ravindran, "Iterative approach for optimising coefficient of power, coefficient of lift and drag of wind turbine rotor," *Renew. Energy*, vol. 38, no. 1, pp. 83–93, Feb. 2012, DOI: 10.1016/j.renene.2011.07.006.

[11] M. Bakırcı and S. Yılmaz, "Theoretical and computational investigations of the optimal tip-speed ratio of horizontal-axis wind turbines," *Eng. Sci. Technol. Int. J.*, **vol. 21, no. 6,** pp. 1128–1142, Dec. 2018, DOI: 10.1016/j.jestch.2018.05.006.

[12] T. D. Oliveira, L. A. Tofaneli, and A. Á. B. Santos, "Combined effects of pitch angle, rotational speed and site wind distribution in small HAWT performance," *J. Braz. Soc. Mech. Sci. Eng.*, vol. 42, no. 8, p. 425, Aug. 2020, DOI: 10.1007/s40430-020-02501-4.